Journal for
Electrochemistry and
Plating Technology

JEPT

Edited by: DGO-Fachausschuss Forschung – Hilden / Germany

Electrochemical Investigation on the Corrosion Behaviour of Mg-Al-Zn-Mn (GA9) Alloy in Sodium Chloride Medium

The corrosion behavior of Mg-Al-Zn-Mn (GA9) alloy in sodium chloride solutions was studied over a range of concentrations and solution temperatures by electrochemical techniques like potentiodynamic polarization (PP) and electrochemical impedance spectroscopy (EIS). The studies were carried out in solutions with NaCl of concentrations between 0.1M - 2M; and at different temperatures in the range of 30 °C - 50 °C. The studies have revealed that the corrosion rate of GA9 magnesium alloy increases with the increase in temperature and also with the increase of NaCl concentration in the medium. Activation parameters like activation energy, enthalpy of activation and entropy of activation for evaluation of the corrosion process were calculated. The results from both the techniques are...

Received: 2014-02-04
Received in revised form: 2014-04-10
Accepted: 2014-04-18

Keywords: GA9 Magnesium,
EIS, Polarization, SEM

By S. Shetty, J. Nayak and A. N. Shetty

DOI:
10.12850/ISSN2196-0267.JEPT3343

LEUZE VERLAG
seit 1902

Electrochemical Investigation on the Corrosion Behaviour of Mg-Al-Zn-Mn (GA9) Alloy in Sodium Chloride Medium

S. Shetty[1], J. Nayak[2] and A. N. Shetty[1]

[1] *Department of Chemistry, National Institute of Technology Karnataka, Surathkal, Post Srinivasnagar, Mangalore-575025 Karnataka, India*

[2] *Department of Metallugy and Materials Engineering, National Institute of Technology Karnataka, Surathkal, Post Srinivasnagar, Mangalore-575025 Karnataka, India*

Keywords: GA9 Magnesium, EIS, Polarization, SEM
Paper: Received: 2014-02-04 / Received in revised form: 2014-04-10 / Accepted: 2014-04-18
DOI: 10.12850/ISSN2196-0267.JEPT3343

The corrosion behavior of Mg-Al-Zn-Mn (GA9) alloy in sodium chloride solutions was studied over a range of concentrations and solution temperatures by electrochemical techniques like potentiodynamic polarization (PP) and electrochemical impedance spectroscopy (EIS). The studies were carried out in solutions with NaCl of concentrations between 0.1M - 2M; and at different temperatures in the range of 30 °C - 50 °C. The studies have revealed that the corrosion rate of GA9 magnesium alloy increases with the increase in temperature and also with the increase of NaCl concentration in the medium. Activation parameters like activation energy, enthalpy of activation and entropy of activation for evaluation of the corrosion process were calculated. The results from both the techniques are in good agreement with each other. The alloy surface morphology was studied before and after corrosion using scanning electron microscopy (SEM).

1. Introduction

Magnesium alloys are the most widely used structural metal alloy all over the world for weight-critical applications, because of their high strength to weight ratio, low density, good damping characteristics, appreciably good castability, recyclability and excellent machinability [1-3]. Despite their advantageous properties, the use of magnesium and its alloys is limited, principally due to their very high corrosion susceptibility. There are two main reasons for the lower corrosion resistance of magnesium alloys; the first reason is the internal galvanic corrosion of the anodic primary α - phase in contact with the second phases (β - phases) or impurities; the second reason is that the hydroxide film on magnesium is much less stable than passive films that form on metals such as aluminium alloys and stainless steels [4]. There are data available in literature, establishing pure magnesium corrosion behaviour in variety of media, like chloride [5], sulphate [6,7], engine coolants as ethylene glycol [8,9], etc., or in the understanding of the mechanism of the magnesium anodic dissolution in corrosive media [10,11]. The influence of the additives, alloying elements and changes in microstructure on the corrosion behaviour of magnesium and its alloys has been established by studying the corrosion process of a variety of magnesium alloys [12 - 18]. Magnesium-alumin-

ium-zinc (Mg-Al-Zn) alloys and magnesium-aluminium-zinc -manganese (Mg-Al-Zn-Mn) alloys are widely used in the automotive field. Due to the presence of aluminium, GA9, which is a Mg-Al-Zn-Mn alloy, acquires a better castability and an increase of ambient tensile, compressive and fatigue strength [19]. Manganese could improve the corrosion resistance of Mg-Al alloy and Mg-Al-Zn alloy by removing iron and other heavy metal elements to avoid the formation of harmful intermetallic compounds. Besides, manganese could refine the grain size and improve the welding properties of the magnesium alloys [20]. Many of these alloys parts find applications outdoor, where they get exposed to open atmosphere and often encounter aqueous salt environments (acidic rain, salts in polluted humid air and road splash for automobile parts) which are potential corrosive media, causing severe corrosion of the alloy. A good understanding of the corrosion behaviour of the alloy in aqueous salt environment like aqueous chloride solutions is essential in the development of any corrosion controlling measure. So the present study is intended to explore the corrosion behaviour of Mg-Zn-Al-Mn alloy having a specific composition in a medium with variable concentration of chloride ions, at different temperatures using electrochemical corrosion monitoring techniques.

2. Experimental

2.1 Material

Experiments were performed with a specimen of Mg-Al-Zn-Mn (GA9) alloy with a percentage composition given in the Table 1. The working electrode from GA9 alloy was in the form of a rod machined into a cylindrical form embedded in epoxy resin leaving an active surface area of 0.6363 cm^2. These coupons were abraded as per standard metallographic practice, belt grinding followed by polishing on emery papers of grade from 600 till 2000, finally on polishing wheel using legated alumina abrasive to obtain a mirror finish. Then the samples were degreased with acetone and dried before immersing in the experimental medium (electrolyte).

Tab. 1: The composition of the Mg-Al-Zn-Mn alloy specimens (% by weight)

Element	Al	Zn	Mn	Ni	Cu	Fe	Si	Mg
Composition (%)	8.80	0.71	0.19	<0.001	0.002	0.001	0.029	Bal.

2.2 Electrolytes

Sodium chloride and bidistilled water were used for preparing the test solutions having concentration of 0.1 M, 0.5 M, 1 M, 1.5 M and 2 M. The corrosion tests were carried out at temperatures 30°C, 35°C, 40°C, 45°C and 50°C (±0.5°C), by putting the corrosion cell in a calibrated thermostat.

2.3 Electrochemical measurements

Electrochemical measurements were carried out using an electrochemical work station, Gill AC having ACM instrument Version 5 software. The experimental corrosion cell employed was a conventional three-electrode Pyrex glass cell with a platinum counter electrode, a saturated calomel electrode (SCE) as reference and the GA9 magnesium alloy specimen as the working electrode. All the potential values reported are referred to the SCE. The polarization studies were carried out immediately after the EIS studies on the same exposed electrode surface without any additional surface treatment.

2.3.1 Potentiodynamic polarization studies

Finely polished GA9 magnesium alloy, sealed by epoxy resin with exposure surface of 0.6363 cm^2 as working electrode was exposed to the corrosion medium of different concentrations of NaCl (0.1 M to 2.0 M) at different temperatures (30 °C to 50 °C) and allowed to establish a steady state open circuit potential (OCP). The potentiodynamic current - potential curves were recorded by polarizing the specimen to -250 mV cathodically and +250 mV anodically with respect to open circuit potential (OCP) at scan rate of 1 mV s^{-1}.

2.3.2 Electrochemical impedance spectroscopy studies (EIS)

EIS measurements were carried out at steady open circuit potential (OCP) by the application of a periodic small amplitude (10 mV) ac voltage signal with a wide spectrum of frequency ranging from 100 kHz to 0.01 Hz. The impedance data were analysed using Nyquist plots. The charge transfer resistance, R_{ct} was extracted from the diameter of the capacitive loop in Nyquist plot.

In all the above measurements, at least three similar results were considered and their average values are reported.

2.4 Scanning electron microscopy (SEM) analysis

The surface morphology of the GA9 alloy specimens in the presence and absence of the corrosive medium was established by recording SEM images using JEOL JSM-6380LA.

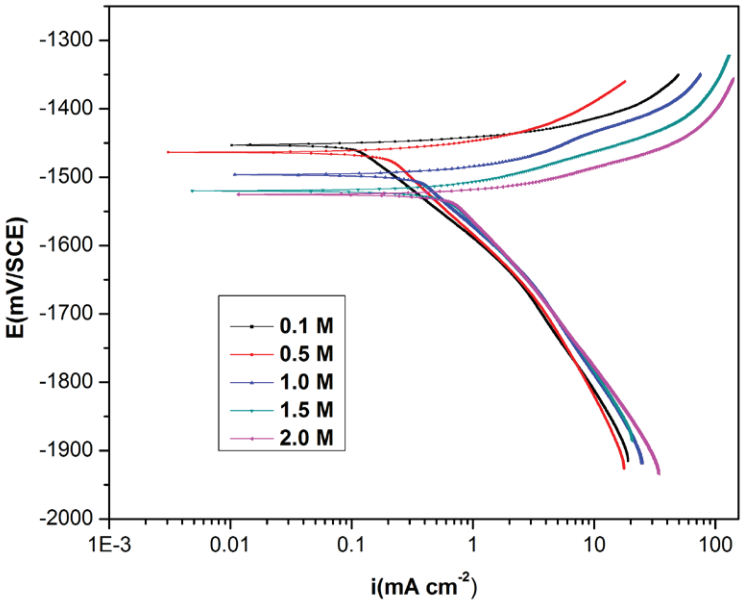

Fig. 1: Potentiodynamic polarization curves for the corrosion of GA9 magnesium alloy in different concentrations of the NaCl solutions at 40°C

3. Results and discussion

3.1 Potentiodynamic polarization measurement

The polarization measurements of GA9 magnesium alloy specimen were carried out in NaCl media of varying concentrations and at different solution temperatures. The potentiodynamic polarization curves for the corrosion of GA9 magnesium alloy in NaCl of different concentrations at 40°C are represented in Figure 1. It is observed from Figure 1 that the polarization curves are shifted to the higher current density region with the increase of the chloride ion concentration, indicating an increased rate of corrosion. Similar plots have been obtained at other temperatures also. The anodic polarization curves are assumed to represent anodic oxidation of magnesium. The shape of these anodic polarization curves indicate nonlinear behaviour in the Tafel region. The appearance of an anodic plateau in solution suggests a pseudo-passivation step [21]. However, the cathodic branch of polarization curves showed linear behaviour in the Tafel region and thought to represent cathodic hydrogen evolution through the reduction of water. The corrosion current density (i_{corr}) was deduced from the extrapolation of cathodic branch of the Tafel plots to the corrosion potential.

The potentiodynamic polarization parameters like corrosion potential (E_{corr}), corrosion current density (i_{corr}), cathodic slopes (b_c) and corrosion rate (υ_{corr}) are calculated from Tafel plots. The calculated parameters for GA9 magnesium alloy in different concentrations of NaCl, at different temperatures are presented in Table 2. The corrosion rate is calculated using Equation 1.

Equation 1:

$$\upsilon_{corr}(mmy^{-1}) = \frac{3270 \times M \times i_{corr}}{\rho \times Z}$$

where, 3270 is a constant that defines the unit of corrosion rate, i_{corr} is the corrosion current density in A cm^{-2}, ρ is the density of the corroding material, 1792 kg m^{-3}, M is the atomic mass of the metal, and Z is the number of electrons transferred per metal atom [22].

It is evident from the data summarized in the Table 2 that the corrosion rate of GA9 magnesium alloy increases with the increase in the concentration of chloride ions in the solution, indicating the strong influence of the corrosive strength of the media on the rate of alloy corrosion. Chloride has been reported to be a strong corrosive, possessing appreciable influence on the electrochemical behaviour of pure magnesium and some of its alloys [6, 7, 23]. The corrosiveness of chloride ions towards magnesium and its alloys arises from their tendency to cause surface film breakdown by transforming the deposited corrosion product, $Mg(OH)_2$, to easily soluble $MgCl_2$. The corrosion potential (E_{corr}), shifts towards more negative (more active) values with the increase in the concentration of chloride ions in the corrosion media. Similar trend of a more negative E_{corr} associated with a higher corrosion rate had been reported by Baril and Pebere [7] for pure magnesium corrosion in sulphate medium and by Zhao [24] for corrosion of magnesium zinc alloy in chloride medium. However, this behaviour cannot be concluded as a phenomenon, as in majority of studies no such direct relation between E_{corr} and corrosion rate had been reported [25]. The slopes of the Tafel branches change with the change in the chloride ion concentration of the medium, without any modifications in overall shape. This fact indicates that the strength of the corrosive medium strongly influences kinetics of the cathodic hydrogen evolution and the anodic metal dissolution reactions without altering the mechanism of alloy corrosion.

Tab. 2: Electrochemical polarization parameters for the corrosion of GA9 magnesium alloy in different concentrations of NaCl at different temperatures

Molarity of NaCl	Temperature (°C)	$-E_{corr}$ (mV vs SCE)	$-b_c$ (mV dec^{-1})	i_{corr} (mA cm^{-2})	ν_{corr} (mm y^{-1})
0.1M	30	1449	149	0.074	1.665
	35	1445	157	0.088	1.980
	40	1450	164	0.108	2.430
	45	1465	169	0.139	3.127
	50	1472	173	0.189	4.252
0.5M	30	1451	152	0.164	3.690
	35	1473	158	0.179	4.027
	40	1466	167	0.193	4.342
	45	1490	171	0.298	6.705
	50	1497	175	0.376	8.460
1.0M	30	1474	156	0.264	5.940
	35	1495	162	0.299	6.727
	40	1496	169	0.361	8.122
	45	1496	177	0.508	11.430
	50	1501	179	0.665	14.962
1.5M	30	1497	169	0.376	8.459
	35	1499	173	0.436	9.809
	40	1519	181	0.552	12.419
	45	1520	195	0.737	16.582
	50	1529	210	0.998	22.455
2.0M	30	1524	192	0.448	10.055
	35	1525	195	0.546	12.285
	40	1529	206	0.725	16.312
	45	1530	213	1.007	22.657
	50	1535	222	1.248	28.079

The corrosion of magnesium alloy normally proceeds by an electrochemical reaction with water to produce magnesium hydroxide and molecular hydrogen (H_2) [26, 27]. The overall reaction is:

Equation 2:

$$Mg + 2H_2O \rightarrow Mg(OH)_2 + H_2$$

The anodic dissolution of magnesium has been proposed to be consisting of oxidation of magnesium into monovalent Mg^+ ions and divalent Mg^{2+} ions as represented by the following reactions [12]:

Equation 3:

$$Mg \rightarrow Mg^+ + e^-$$

Equation 4:

$$Mg \rightarrow Mg^{2+} + 2e^-$$

The standard electrode potential of magnesium is −2.38 V(/SHE), but the steady state working potential is about −1.5 V(/SHE). The difference in potential has been attributed to the formation of $Mg(OH)_2$ film on the metal surface [28]. As represented in the equations 3 and 4, the anodic dissolution of magnesium and its alloys involves two oxidation processes. At more active potentials around −2.78 V (vs SCE), magnesium is oxidized to monovalent magnesium ion and at slightly higher potentials of −1.56 V (vs SCE), oxidation of magnesium to divalent magnesium ion takes place in parallel with the former oxidation [11]. The monovalent magnesium ion being unstable undergoes oxidation to divalent magnesium ion through a series of reactions involving unstable intermediates like magnesium hydride as shown in equations below:

Equation 5:

$$Mg^+ + 2H^+ + 3e^- \rightarrow MgH_2$$

Equation 6:

$$MgH_2 + 2H_2O \rightarrow Mg^{2+} + 2OH^- + 2H_2$$

Equation 7:

$$Mg^{2+} + 2OH^- \rightarrow Mg(OH)_2$$

Equation 8:

$$2Mg^+ + 2H_2O \rightarrow Mg^{2+} + Mg(OH)_2 + H_2$$

GA9 magnesium alloy is a dual phase alloy with a typical microstructure of having a primary α-phase and a divorced eutectic β-phase, distributed along the grain boundaries [2]. The α-Mg matrix is an α-Mg-Al-Zn solid solution with the same crystal structure as pure magnesium and the β-phase is with a composition of $Mg_{17}Al_{12}$. The α-Mg matrix corrodes due to its very negative free corrosion potential. The β-phase of $Mg_{17}Al_{12}$ is cathodic to the α-Mg matrix and tends to accelerate the corrosion rate by micro galvanic coupling between anodic α-Mg phase and cathodic β-$Mg_{17}Al_{12}$ phase [15, 18, 29 -33]. However, the β-$Mg_{17}Al_{12}$ phase may act as a barrier against corrosion propagation if it is in the form of a continuous network [18, 29]. The corrosion of the alloy in the chloride media indicates the discontinuities in the β-phase. According to the reports in the literature, magnesium alloys exhibit higher corrosion resistance than pure magnesium [34]. The improvement of the corrosion behavior of Mg alloys due to the alloying elements has been attributed to a number of factors such as refining of the β-phase and formation of more continuous network, suppression of β-phase formation by forming another intermetallic, which is less harmful to the α-Mg matrix, and added elements may incorporate into the protective film and thus increasing its stability [35–37]. Small additions of Mn have been reported to increase the corrosion resistance of magnesium alloys and reduce the effects of metallic impurities [38, 39].

3.2 Electrochemical impedance spectroscopy (EIS)

The corrosion study of GA9 magnesium alloy specimen was investigated by EIS method in various concentrations of sodium chloride at different temperatures. The typical Nyquist plots for the corrosion of GA9 specimen in chloride solutions of different concentrations at 40 °C are shown

in Figure 2. Similar plots were obtained at other temperatures also. The Nyquist plots are characterized by a capacitive loop, extended from high frequency (HF) to low frequency (LF) range, an inductive loop in the low frequency region (LF) range and a tail at the medium frequency (MF) range. The HF capacitive loop is usually due to the charge transfer resistance and double layer capacitance at the metal-solution interface. The inductive behavior at low frequencies is associated with high concentration of Mg ions on relatively film-free areas [40, 41] or due to the presence of adsorbed surface species such as $Mg(OH)^+$, $Mg(OH)_2$ and Mg^+ [40, 42]. Also the tail in the Nyquist plot in the medium frequency range correlates with the breakage of native corrosion product film [43]. The charge transfer resistance (R_{ct}) and the double layer capacitance (C_{dl}) are deduced from the analysis of a higher frequency capacitive loop [8, 44].

The corrosion current density is calculated using the Stern Geary Equation [17]:

Equation 9:

$$i_{corr} = \frac{b_a b_c}{2.303(b_a + b_c)R_{ct}}$$

From Figure 2 it is clear that the diameter of the capacitive loop decreases with the increase in the concentration of the chloride ions, indicating the decrease in R_{ct} value and increase in the corrosion rate. The results of EIS measurements are listed in the Table 3. These results are well in agreement with the results obtained from potentiodynamic polarization measurements.

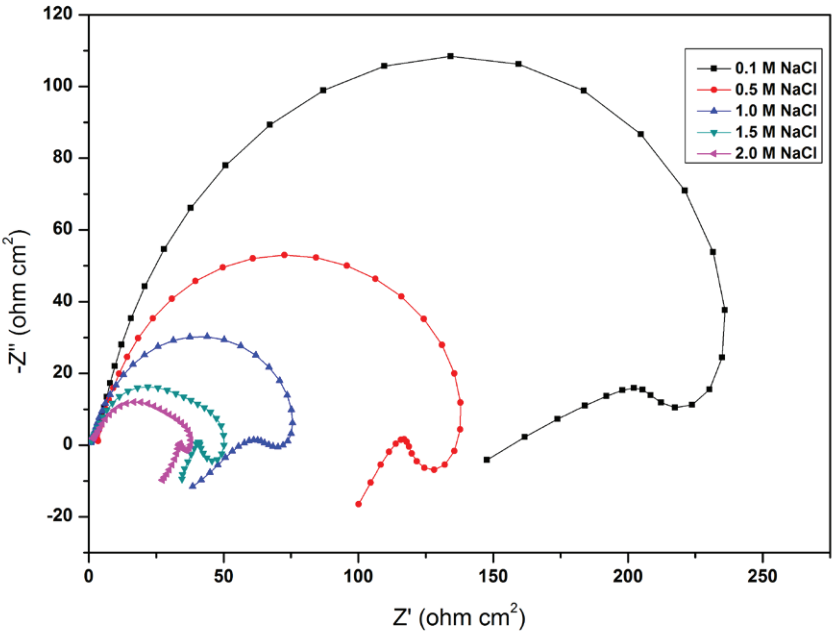

Fig. 2: Nyquist plots for the corrosion of GA9 magnesium alloy in different concentrations of NaCl solutions at 40°C

Tab. 3: Impedance parameters for the corrosion of GA9 magnesium alloy in different concentrations of NaCl at different temperatures

Molarity of NaCl	Temperature (°C)	R_{ct} (Ω cm^2)	C_{dl} (μF cm^{-2})	ν_{corr} (mm y^{-1})
0.1M	30	362.6	11.27	1.619
	35	302.1	11.42	1.935
	40	245.3	15.20	2.385
	45	185.3	23.47	3.172
	50	132.5	28.93	4.409
0.5M	30	162.6	26.16	3.592
	35	146.7	27.22	3.982
	40	136.2	28.53	4.297
	45	84.7	35.18	6.929
	50	72.7	40.27	8.054
1.0M	30	103.3	33.42	5.669
	35	83.6	34.98	6.997
	40	73.7	39.86	7.942
	45	50.9	66.71	11.497
	50	37.8	77.61	15.502
1.5M	30	67.9	41.59	8.617
	35	60.9	61.11	9.630
	40	48.7	69.76	12.037
	45	34.5	89.52	16.987
	50	26.9	107.41	21.779
2.0M	30	58.5	58.01	10.012
	35	46.3	65.13	12.644
	40	37.6	83.92	15.592
	45	26.4	109.41	22.207
	50	21.5	123.22	27.518

The impedance results are analyzed using equivalent circuit models. The circuit fitment was done by the ZSimpWin software of version 3.21. Figure 3 shows the simulation of the impedance data

points. The equivalent circuit modelling of the electrochemical behaviour of the interface as shown at the right hand corner of Figure 3 comprises five circuit elements, R_e represents the electrolyte resistance, R_c stands for the charge transfer resistance. The capacitive loop appears as depressed semicircle, as a result of frequency dispersion arising due to inhomogeneity of the solid surface [27]. The constant phase element (CPE) is substituted for the ideal capacitive element to account for the unevenness and porosity of the electrode surface. The impedance of the constant phase is described by the expression:

Equation 10:

$$Z_Q = Y_0^{-1}(j\omega)^{-n}$$

where Y_0 is the CPE constant, ω is the angular frequency (in rad s^{-1}), $j^2 = -1$, is the imaginary number and n is a CPE exponent that is a measure of the heterogeneity or roughness of the surface. If n = 1, equation (7) becomes impedance of pure capacitor; if n = 0, CPE acts as a pure resistor [10].

3.3. Effect of temperature

The effect of temperature on the corrosion rate of GA9 magnesium alloy was studied by measuring the corrosion rates at different temperature between 30°C–50°C. Figures 4 and 5 represent the potentiodynamic polarization curves and Nyquist plots, respectively, at different temperatures for the corrosion of GA9 magnesium alloy sample in 1M NaCl solution. Similar plots were obtained in other concentrations of NaCl solutions also. The Tafel polarization results and EIS results at different temperatures are listed in Tables 2 and 3, respectively. From the Figures 4 and 5, and also from the results presented in Tables 2 and 3, it is seen that the corrosion rate increases with the increase in temperature. This has been attributed to the reduction in hydrogen evolution overpotential with the increase in temperature. The values of b_c and R_{ct} change with the change in temperature, which is indicative of the fact that temperature plays an influential role in the kinetics of the corrosion reactions. However, the basic shape of polarization curves and Nyquist plots remain

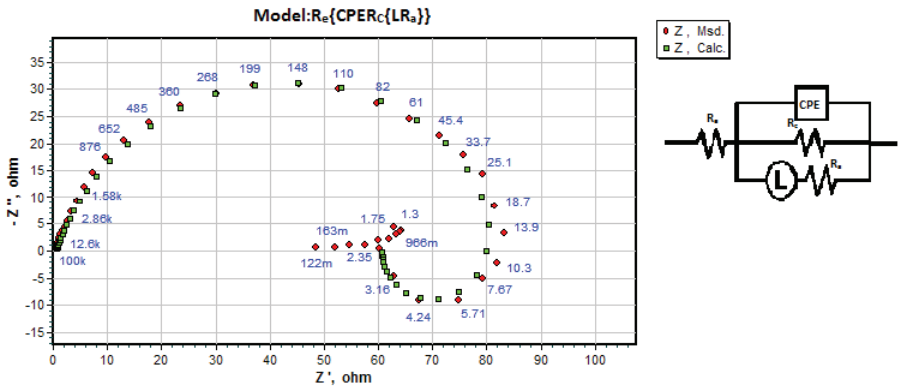

Fig. 3: The equivalent circuit model used to fit the experimental data for the corrosion of GA9 magnesium alloy in 0.5M NaCl solution at 50°C

unaltered, which illustrates that temperature modifies only the rate of alloy corrosion but not the mechanism. Activation energy (E_a) values for the corrosion reaction of GA9 magnesium alloy in NaCl solutions were calculated from the Arrhenius equation (Eq. 11).

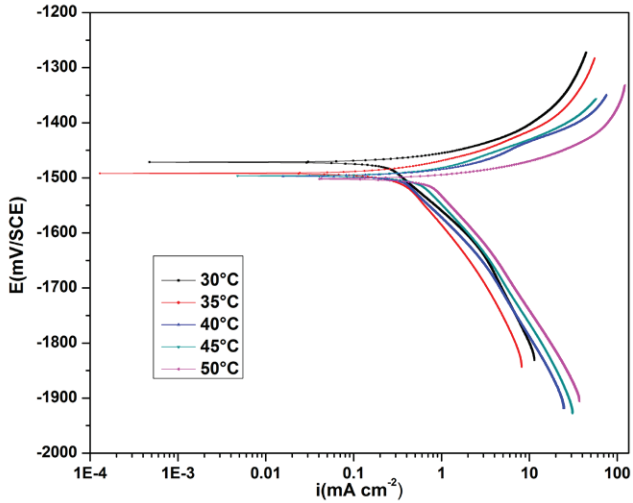

Fig. 4: Potentiodynamic polarization curves for the corrosion of GA9 magnesium alloy in 1M NaCl solution at different temperatures

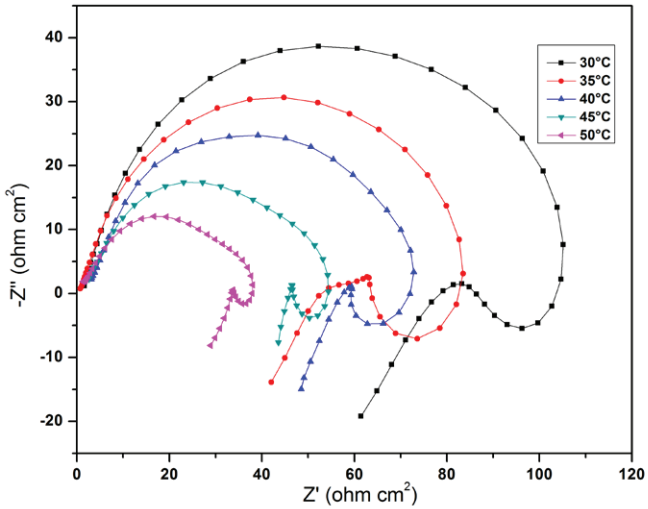

Fig. 5: Nyquist plots for the corrosion of GA9 magnesium alloy in 1M NaCl solution at different temperatures

Equation 11:

$$\ln(\upsilon_{corr}) = B - (E_a / RT)$$

where B is a constant which depends on the metal type, and R is the universal gas constant. The plot of ln (υ_{corr}) vs reciprocal of absolute temperature (1/T) gives a straight line whose slope = $-E_a$ / R, from which the activation energy values for the corrosion process were calculated. The Arrhenius plots for the corrosion of GA9 specimen are shown in Figure 6.

The transition state theory Equation 12 was used for the calculation of enthalpy and entropy of activation ($\Delta H^{\#}$ & $\Delta S^{\#}$).

Equation 12:

$$\upsilon_{corr} = (RT / Nh)\exp(\Delta S^{\#} / R)\exp(-\Delta H^{\#} / RT)$$

Where h is Planck's constant, and N is Avagadro's number and R is the ideal gas constant. A plot of ln(υ_{corr}/T) vs 1/T gives a straight line with slope = $-\Delta H^{\#}/R$ and intercept = $\ln(R/Nh) + \Delta S^{\#}/R$. The plots of ln($\upsilon_{corr}$ /T) versus 1/T for the corrosion of GA9 magnesium alloy in different concentrations of sodium chloride is shown in Figure 7.

Tab. 4: Activation parameters for the corrosion of GA9 magnesium alloy in the NaCl solutions

Molarity of NaCl	Ea (KJ mol^{-1})	$\Delta H^{\#}$ (kJ mol^{-1})	$\Delta S^{\#}$ (J mol^{-1} K^{-1})
0.1M	37.86	35.26	-124.86
0.5M	35.12	32.52	-127.73
1.0M	38.57	35.97	-112.20
1.5M	40.22	37.62	-103.73
2.0M	43.35	40.75	-91.68

The activation parameters calculated are listed in the Table 4. The activation energy values indicate that the corrosion of the alloy is controlled by a surface reaction, since the values of the activa-

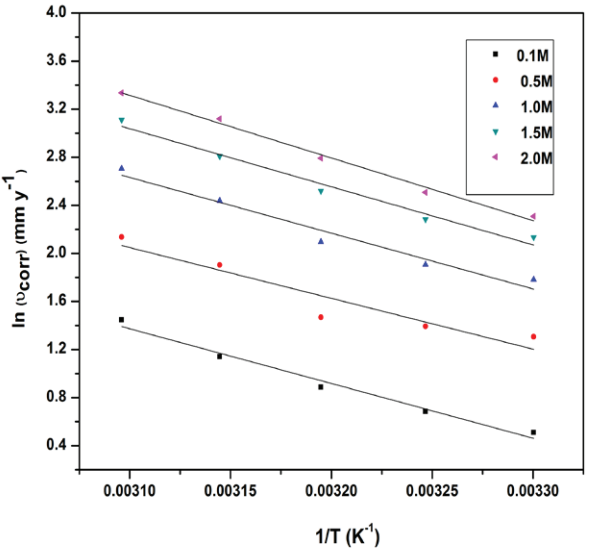

Fig. 6: Arrhenius plots for the corrosion of GA9 magnesium alloy in NaCl solutions

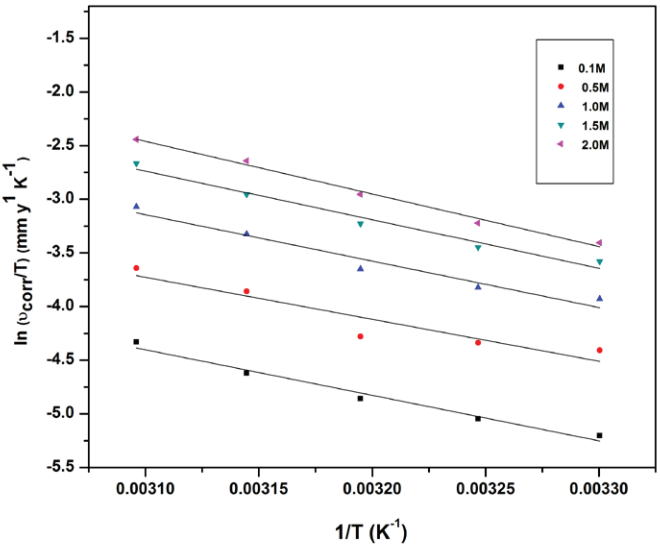

Fig. 7: ln(υ_{corr} / T) vs 1/T plots of for the corrosion of GA9 magnesium alloy in NaCl solutions

tion energy for the corrosion process is greater than 20 kJ mol^{-1} [45]. The entropy of activation is negative. This implies that activated complex in the rate-determining step represents association rather than dissociation, indicating a decrease of randomness taking place on going from the reactants to the activated complex.

3.4. SEM and EDX examinations of the electrode surface

The SEM image of a freshly polished surface of GA9 magnesium alloy sample is given in Figure 8(a), which shows the uncorroded surface with few scratches due to polishing. Figure 8(b) shows

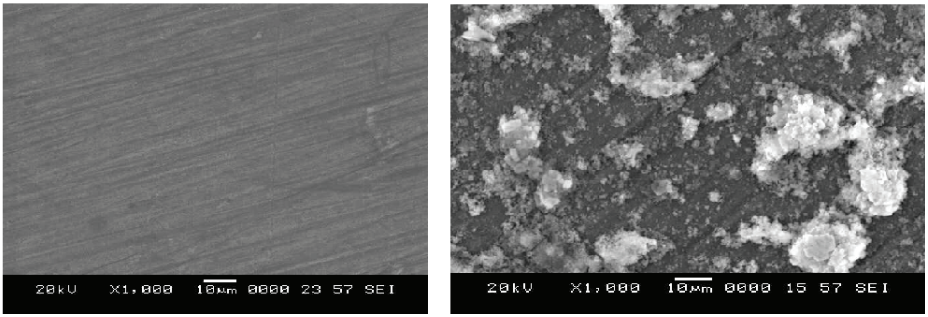

Fig . 8: SEM images of (a) freshly polished surface, (b) corroded surface

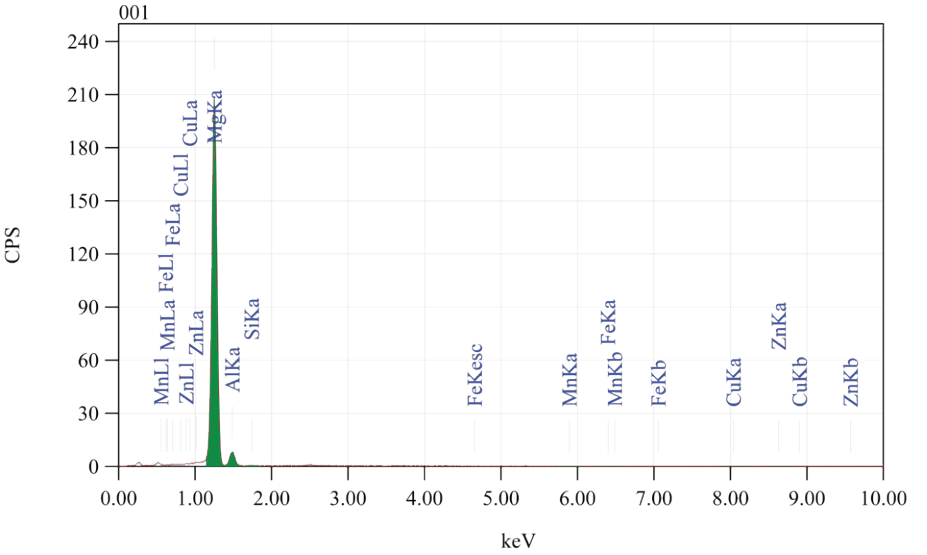

Fig. 9(a): EDX images of a freshly polished surface

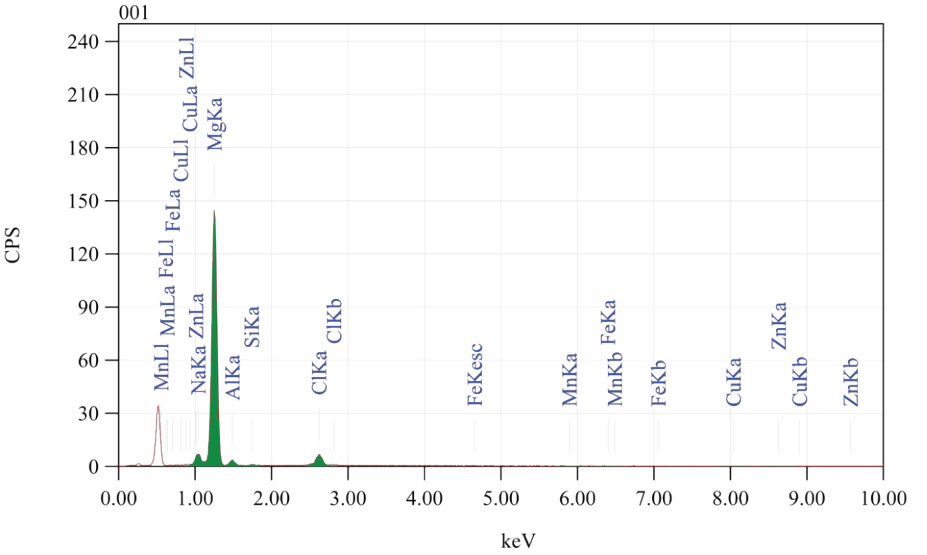

Fig. 9(b): EDX images of the corroded surface

the SEM image of GA9 magnesium alloy surface after immersed for 3 h in 2 M NaCl. The SEM images reveal that the GA9 magnesium alloy specimen not immersed in the chloride solutions is in a better condition having a smooth surface while the surface of the alloy immersed in 2 M NaCl is deteriorated due to the corrosion of the alloy surface.

EDX survey spectra were used to determine the surface composition of the specimens before and after exposure to the sodium chloride solution. Figure 9(a) reveals that fresh surface of the GA9 alloy specimen with an intense peak of Mg. The Figure 9(b) shows that the Mg peaks are considerably suppressed relative to the fresh specimen. Also, a peak for chlorine is observed in Figure 9(b), indicating the presence of chloride on the metal surface as part of the corrosion product.

4. Conclusions

From the above results and discussion, the main conclusions can be summarized in the following points:

- The environmental factors like temperature and chloride concentration of the corrosion media have a remarkable influence on rate of corrosion of GA9 magnesium alloy.
- The results obtained from Tafel polarization curves and electrochemical impedance spectroscopy is in reasonable agreement with each other.
- The corrosion rate of the GA9 alloy under investigations increases with the increase in solution temperature from 30 oC to 50 oC and concentration of the chloride ions from 0.1 M to 2.0 M.
- The corrosion kinetics of GA9 alloy in NaCl medium follows Arrhenius law.

References

[1] C. Blawert, N. Hort, K.U. Kainer, Automotive applications of magnesium and its alloys, Trans. Indian Inst. Met. 57 (2004) 397-408.

[2] F.H. Froes, D. Eliezer, E. Aghion, The Science, Technology, and Applications of Magnesium, JOM. 50 (1998) 30-34.

[3] M. Gupta, N.M.L. Sharon, Magnesium alloys and magnesium composites, John Wiley & Sons, NewJersy, 2011.

[4] S. A. Salman, R. Ichino, M.A.Okido, Comparative electrochemical study of AZ31 and AZ91 magnesium alloy, Int. J. Corros. (2010) doi:10.1155/2010/412129.

[5] G. Song, A. Atrens, D. StJohn, J. Nairn, Y. Li, The electrochemical corrosion of pure magnesium in 1N NaCl, Corros. Sci. 39 (1997) 855-875.

[6] G. Song, A. Atrens, D. StJohn, X. Wu, J. Nairn, The anodic dissolution of magnesium in chloride and sulphate solutions, Corros. Sci. 39 (1997) 10-11.

[7] G. Baril, N. Pebere, The corrosion of pure magnesium in aerated and deaerated sodium sulphate solutions, Corros. Sci. 43 (2001) 471-484.

[8] G. Song, D. StJohn, Corrosion behaviour of magnesium in ethylene glycol, Corros. Sci. 46 (2004) 1381-1399.

[9] G. Song, D. StJohn, Corrosion of magnesium alloys in commercial engine coolants, Mater. Corros. 56 (2005) 15-23.

[10] J.H. Greenblatt, A mechanism for the anodic dissolution of magnesium, J. Electrochem. Soc. 103 (1956) 539-543.

[11] M.G. Lopez, B. Natta, Evidence of two anodic processes in the polarization curves of magnesium in aqueous media. Corrosion. 712 (2001) 5006-5015.

[12] M. Baghni, Y. Wu, J. Li, W. Zhang, Corrosion behaviour of magnesium and magnesium alloys, Trans. Nonferrous. Met. Soc. China. 14 (2004) 1-10.

[13] Y. Fan, G. Wu, C. Zhai, Influence of cerium on the microstructure, mechanical properties and corrosion resistance of magnesium alloy, Mater. Sci. Eng. A 433 (2006) 208-215.

[14] S. Izumi, M. Yamasaki, Y. Kawamura, Relation between corrosion behaviour and microstructure of Mg-Zn-Y alloys prepared by rapid solidification at various cooling rates, Corros. Sci. 51 (2009) 395-402.

[15] G. Song, A. Atrens, M. Dargusch, Influence of microstructure on the corrosion of diecast AZ91,D Corros. Sci. 41 (1999) 249-273.

[16] M. Sun, G. Wu, W. Wang, W. Ding, Effect of Zr on the microstructure, mechanical properties and corrosion resistance of Mg–10Gd–3Y magnesium alloy, Mat. Sci. Eng. A. 523 (2009) 145-151.

[17] D.K. Xu, W.N. Tang, L. Liu, Y.B. Xu, E.H. Han, Effect of Y concentration on the microstructure and mechanical properties of as-cast Mg–Zn–Y–Zr alloys, J. Alloys Compd. 432 (2007) 129-134.

[18] M.C. Zhao, M. Liu, G. Song, A. Atrens, Influence of the b-phase morphology on the corrosion of the Mg alloy AZ91, Corros. Sci. 50 (2008) 1939-1953.

[19] G. Song, A. Atrens, X. Wu, B. Zhang. Corrosion behaviour of AZ21, AZ501and AZ91 in sodium chloride. Corros. Sci. 40 (1998) 1769-1791.

[20] Y. Cheng, T. Qin, H. Wang, Z. Zhang, Comparison of corrosion behaviours of AZ31, AZ91, AM60 and ZK60 magnesium alloys, Trans. Nonferrous Met. Soc. China. 19 (2009) 517-524.

[21] G. Song, A. Atrens, D.S. John, X. WU, J. Nairn, The anodic dissolution of magnesium in chloride and sulphate solutions. Corros. Sci. 39 (1997) 1981-2004.

[22] Z. Shi, A. Atrens, An innovative specimen configuration for the study of Mg corrosion. Corros. Sci.53 (2011) 226-246.

[23] L. Wang, T. Shinohara, B. Zhang, Influence of chloride, sulphate and bicarbonate anions on the corrosion behaviour of AZ31 magnesium alloy, J. Alloys Compd. 496 (2010) 500-507.

[24] M.C. Zhao, M. Liu, G. Song, A. Atrens, Influence of pH and chloride ion concentration on the corrosion of Mg alloy ZE41, Corros. Sci. 50 (2008) 3168-3178.

[25] D. Nandini, A. N. Shetty, Electrochemical investigations on the corrosion behaviour of magnesium alloy ZE41 in a combined medium of chloride and sulphate, J. Magnesium and Alloys 1 (2013) 201-209.

[26] L. Wang, B.P. Zhang, T. Shinohara, Corrosion behaviour of AZ91 magnesium alloy in dilute NaCl solutions, Materials and Design. 31 (2010) 857-863.

[27] L.J. Liu, M. Schlesinger, Corrosion of magnesium and its alloys. Corros. Sci. 50, (2009) 1733-1737.

[28] R. Udhayan, D.P. Bhatt, On the corrosion behaviour of magnesium and its alloys using electrochemical techniques, J. Power Sources. 63 (1996) 103-107.

[29] R. Ambat, N.N. Aung, W. Zhou, Evaluation of microstructural effects on corrosion behaviour of AZ91D magnesium alloy, Corros. Sci. 42 (2000) 1433-1455.

[30] R. Ambat, N.N. Aung, W. Zhou, Studies on the influence of chloride ion and pH on the corrosion and electrochemical behaviour of AZ91D magnesium alloy, J. Appl. Electrochem. 30 (2000) 865-874.

[31] N.N. Aung, W. Zhou, Effect of heat treatment on corrosion and electrochemical behaviour of AZ91D magnesium alloy, J. Appl. Electrochem. 32 (2002) 1397-1401.

[32] G. Song, A.L. Bowles, D.H. StJohn, Corrosion resistance of aged die cast magnesium alloy AZ91D, Mater. Sci. Eng. 366 (2004) 74-86.

[33] M. Jonsson, D. Persson, R. Gubner, The initial steps of atmospheric corrosion on magnesium alloy AZ91D, J. Electrochem. Soc. 154 (2007) C684-C691.

[34] W. A. Badawya, N. H. Hilal, M. El-Rabiee, H. Nady, Electrochemical behaviour of Mg and some Mg alloys in aqueous solutions of different pH, Electrochim. Acta 55 (2010) 1880–1887.

[35] W. Guohua, F. Yu, G. Hongtao, Z. Chunquan, Z.Y. Ping, The effect of Ca and rare earth elements on the microstructure, mechanical properties and corrosion behaviour of AZ91D, Mater. Sci. Eng. A 408 (2005) 255 - 263.

[36] F. Yu, W. Guohua, Z. Chunquan, Influence of cerium on the microstructure, mechanical properties and corrosion resistance of magnesium alloy, Mater. Sci. Eng. A 433 (2006) 208 - 215.

[37] F. Yu, W. Guohua, G. Hongtao, L. Guanqun, Z. Chunquan, Influence of lanthanum on the microstructure, mechanical property and corrosion resistance of magnesium alloy, J. Mater. Sci. 41 (2006) 5409 - 5417.

[38] B.E. Carlson, J.W. Jones, The metallurgical aspects of the corrosion behaviour of cast Mg–Al alloys, in: Light Metals Processing and Applications, METSOC Conference, Quebec, 1993.

[39] I.J. Polmer, Physical Metallurgy of Magnesium alloys, DGM Informationsgesellschaft, Oberursel, Germany, 1992, p. 201.

[40] J. Chen, J. Wang, E. Han, J. Dong, W. Ke, AC impedance spectroscopy study of the corrosion behaviour of an AZ91 magnesium alloy in 0.1 M sodium sulphate solution, Electrochim. Acta. 52 (2007) 3299-3309.

[41] G. Baril, N. Pebere, The corrosion of pure magnesium in aerated and deaerated sodium sulphate solutions, Corrosion Science. 43 (2001), 471-484.

[42] W.A. Badway, N.H. Hilal, M.E. Rabiee, H. Nady, Electrochemical behaviour of Mg and Mg alloys in aqueous solutions of different pH, Electrochim. Acta. 55 (2010), 1880-1887.

[43] D. Song, A. Ma, J. Jiang, P. Lin, D. Yang, J. Fan, Corrosion behaviour of equal-channel-angular-pressed pure magnesium in NaCl aqueous solution, Corros. Sci. 52 (2010) 481-490.

[44] H. Ardelean, I. Frateur, P. Marcus, Corrosion protection of magnesium alloys by cerium, zirconium and niobium-based conversion coatings, Corros Sci. 50 (2008) 1907-1918.

[45] M. Bouklah, B. Hammouti, M. Benkaddour, T. Benhadda, Thiophene derivatives as effective inhibitors for the corrosion of steel in 0.5 M H2SO4. J. Appl. Electrochem. 35 (2005), 1095-1101.

Corresponding author:

Prof. Dr. A. Nityananda Shetty
Department of Chemistry, National Institute of Technology Karnataka, Surathkal, Post Srinivasnagar, Mangalore-575025 Karnataka, India
Email: nityashreya@gmail.com

Authors:

Jagannath Nayak
Department of Metallugy and Materials Engineering, National Institute of Technology Karnataka, Surathkal, Post Srinivasnagar, Mangalore-575025 Karnataka, India
Email: nityashreya@gmail.com

Sudarshana Shetty
Department of Chemistry, National Institute of Technology Karnataka, Surathkal, Post Srinivasnagar, Mangalore-575025 Karnataka, India

CONTACT:

EUGEN G. LEUZE VERLAG KG
Ralf Schattmaier
Karlstraße 4
88348 Bad Saulgau
Germany

Email: ralf.schattmaier@leuze-verlag.de
Phone: +49 0 7581 4801-12
Fax: +49 0 7581 4801-10